TISSUE ENGINEERING: Part C
Volume 23, Number 9, 2017

DOI: 10.1089/ten.tec.2017.0228

termis
Tissue Engineering
& Regenerative Medicine
International Society

METHODS ARTICLE

Arthroscopic Airbrush-Assisted Cell Spraying for Cartilage Repair: Design, Development, and Characterization of Custom-Made Arthroscopic Spray Nozzles

Koen Dijkstra, MSc,[1] Jan Hendriks, MSc,[2] Marcel Karperien, PhD,[2] Lucienne A. Vonk, PhD,[1] and Daniël B.F. Saris, MD, PhD[1,3,4]

Introduction: Airbrush-assisted cell spraying would facilitate fully arthroscopic filling of cartilage defects, thereby providing a minimally invasive procedure for cartilage repair. This study provides the development and characterization of custom-made spray nozzles that could serve as a foundation for the development of a BioAirbrush, a platform technology for the arthroscopic application of (cell laden) hydrogels.
Materials and Methods: Custom-made spray nozzles were designed and produced with 3D printing technology. A commercially available spraying system was used for comparison. Sprays were characterized based on spray angle, cone width, droplet size, velocity, and density. This was performed with conventional and high-speed imaging. Furthermore, cell survival of chondrocytes and mesenchymal stromal cells, as well as the chondrogenic capacity of chondrocytes after spraying were evaluated.
Results: Changing nozzle design from internal to external mixing significantly increased cell survival after spraying. Custom-made spray nozzles provide larger droplets compared to the current commercially available technology, potentially improving cell survival. Sufficient mixing of two gel components was confirmed for the custom-made nozzles. Overall, custom-made nozzles improved cell survival after spraying, without significantly affecting the chondrogenic capacity of the cells.
Conclusions: This study provides a platform for the development of a BioAirbrush for spray-assisted cell implantations in arthroscopic cartilage repair procedures. Evaluation of the fundamental characteristics of a spray as well as a study of cell survival after spraying have further expanded the knowledge regarding cell spraying for cartilage repair. Nozzle design and air pressure characteristics are essential parameters to consider for the clinical implementation of spray-assisted cell implantations.

Keywords: cartilage repair, cell spraying, arthroscopic, mesenchymal stromal cells, hydrogels, cell therapy

Introduction

Treatment of knee cartilage defects prevents further progression of articular cartilage damage and allows patients to return to their daily activities, including sports.[1,2] Autologous chondrocyte implantation (ACI) has shown to be a successful procedure for larger defects (>2.5 cm^2), with sustaining benefits up to 20 years.[3–5] However, downsides include the requirement of two surgical procedures, relatively high costs, and the need for a mini-arthrotomy. A previous study has shown that cell viability in third-generation ACI is severely hampered by performing this procedure arthroscopically, because of manipulation of the implant.[6] Besides, it is striking that the main improvements in the field of ACI have been gained in finding the perfect combination of cells and biomaterials, while improvements in surgical instrumentation have been largely neglected.

Recently, we have proposed arthroscopic airbrush-assisted cell implantation as a new strategy to improve

[1]Department of Orthopedics, University Medical Center Utrecht, Utrecht, The Netherlands.
[2]Department of Developmental BioEngineering, University of Twente, Enschede, The Netherlands.
[3]MIRA Institute for BioMedical Technology and Technical Medicine, University of Twente, Enschede, The Netherlands.
[4]Department of Orthopedics, Mayo Clinic, Rochester, Minnesota.

cartilage repair.[7] Cell spraying with an arthroscopic airbrush would facilitate fully arthroscopic filling of cartilage defects, layer by layer. This method could support the recent shift toward less invasive one-stage procedures.[8–12] *In vivo* cell spraying has been applied before in other fields of medicine, such as in the treatment of burn wounds,[13–15] ulcers,[16,17] or seeding of tubular constructs for tracheal tissue engineering.[18] However, currently available commercial spray instruments, made for spraying fibrin glue, are not suitable for arthroscopic use. These instruments are associated with limited arthroscopic maneuverability, the occurrence of device clogging, or destructive effect on cell survival. Hence for implementation of arthroscopic airbrushing in clinical setting, current devices need adaptation.

This study involves the development and characterization of two custom-made spray nozzles that could serve as a foundation for the development of a BioAirbrush, an arthroscopic instrument for cell implantations in cartilage repair procedures. To study the feasibility of spraying cells with these custom-made nozzles, cell survival and chondrogenic potential after spraying were studied.

Materials and Methods

Development of custom-made spray nozzles

Custom-made nozzle designs were created using 3D computer-aided design (3D CAD) software (Autodesk Fusion 360, Student license) (Fig. 1). Previous experimental experience[7,19] and a patent search into fibrin spraying nozzles were used as a starting point for the new designs. An online 3D printing service platform, 3Dhubs, was used to find a manufacturer. MultiJet printing with Visijet M3 Crystal was chosen because of its combination of high printing resolution and biocompatibility (class VI material classification). This material has already been shown to be suitable for production of microfluidic devices for biological applications.[20,21]

Fluid dynamic analysis: spray pattern characterization

To visualize the spray with conventional photography, a setup with a Digital Single Lens Reflex (DSLR) camera (Nikon D750), a black background, and an external light source was used. Illumination of the spray was directed from the side through fiberglass optics. A syringe pump (Harvard Apparatus PHD 2000) and a pressure regulator (WIKA Fein-Druckmeβgerät) were used to ensure stable flow of fluid (demi-water) and air. The continuous burst mode option (C_H) of the D750 was used to acquire images at a frame rate of 6.5 fps. Fifteen to twenty photographs were made for each nozzle. Chosen parameters were air pressure, 0.6 bar, and fluid flow, 2.4 mL/min. Short videos were created by combining the images into Graphics Interchange Format (GIF) files using PicGif (MacOS software) (see Supplementary Videos S1–S3; Supplementary Data are available online at www.liebertpub.com/tec).

Furthermore, images were analyzed using ImageJ (version 1.47v) to measure the cone angle and cone width at 5, 10, and 15 mm distance from the nozzle. Ten randomly chosen images were used for the measurements. Calibration was performed by using the actual diameter of the nozzle visible in the images and angles were measured using the angle tool for the densest part of the spray. The scale bar was used to insert an artificial ruler (5, 10, and 15 mm) in the image (Fig. 2) using Adobe Photoshop CS6, indicating the distance to the nozzle, at which the cone width was measured using the line tool in ImageJ.

Fluid dynamic analysis: droplet characterization

High-speed imaging was used to characterize the spray in terms of droplet size, velocity, and density, as it was previously shown that these parameters might have predictive value regarding cell survival.[19] The experimental setup was adopted from a previous study by Hendriks *et al.*[19] Briefly, the setup captures droplets in sets of two consecutive images with a delay of 1 μs, which enables the calculation of the droplet size

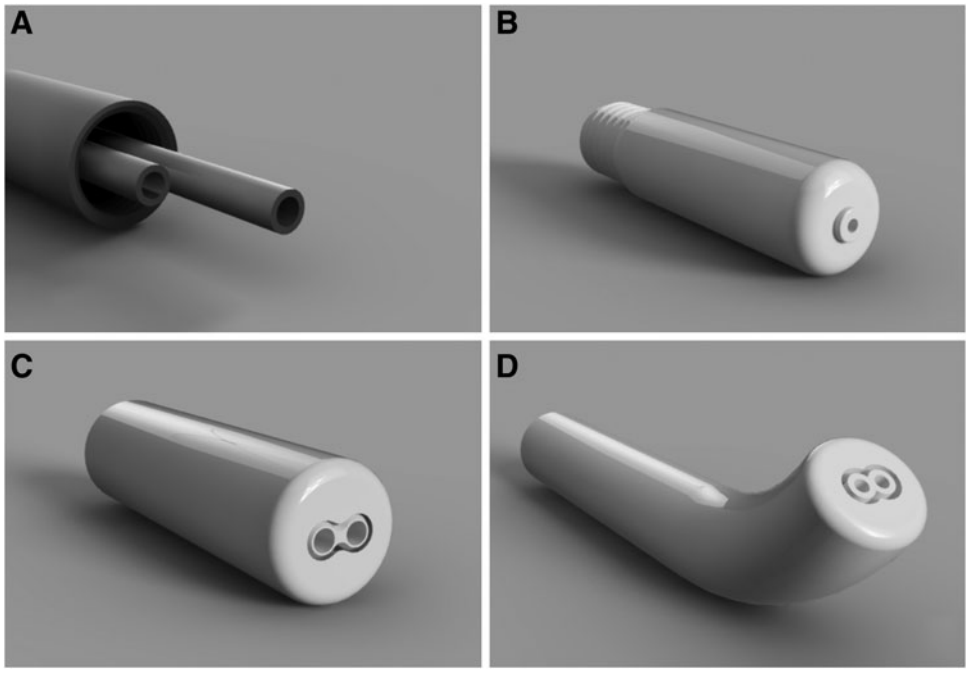

FIG. 1. Nozzle designs. **(A)** Shows the double output channels inside the DuploSpray (Baxter) system. **(B)** Shows the conventional DuploSpray nozzle, whereas **(C, D)** show the designs of the custom-made double barrel and 45° double barrel nozzle, respectively.

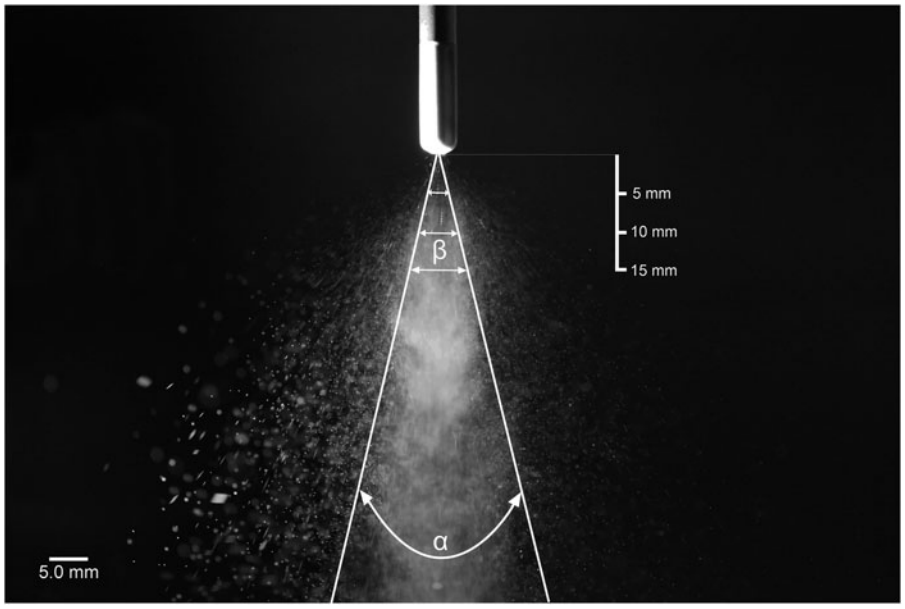

FIG. 2. ImageJ spray characterization analyses. Representative image of the DuploSpray nozzle spray pattern. Similar images were obtained for the other custom-made nozzles. Spray patterns were characterized based on measurements of the cone angle (α) and the cone width (β) at 5, 10, and 15 mm distance from the nozzle.

and velocity. A dual-pulse laser (Quantel Evergreen pulsed ND:Yag laser, 532 nm) was used for brightfield illumination. The pulses were captured by a dual-shutter camera (PCO CCD Sensicam). The delay between the illumination pulses was set to 1 μs using a pulse/delay generator (BNC model 575). A 10× long-distance objective was used at a 10× magnification. To fully characterize droplets at different locations in the spray, measurements were performed at different locations along the *x*-axis [–2, –1, –0.5, 0, 0.5, 1, 2, 3, 5, and 10 mm], where 0 mm is located at the center of the spray.

Measurements were performed at 15 mm distance from the nozzle (*y*-axis). For each location, 429 image pairs were obtained, as seen in the figure (Fig. 3). The droplets were automatically detected using a MATLAB script, detecting only droplets appearing sufficiently sharp, excluding blurred droplets. The script allowed for detection of droplet sizes in a range of 1–100 μm and the downward *x*-*y* Pythagoras translation were used to calculate the droplet velocity. Droplet density was defined as the number of droplets detected in each location of the spray.

Mixing efficiency

Mixing of the two fibrin glue components after spraying with the newly developed 45° double barrel (DB) nozzle was evaluated. The 45°DB nozzle was chosen for this experiment because this was considered the design with the highest potential for arthroscopic use. To evaluate the mixing of the gel, microspheres were added to the components of the fibrin glue. Blue 15 μm microspheres (Triton Dye TRAK, CA) were added to the fibrinogen component (Tisseel; Baxter) and yellow 15 μm microspheres (Triton Dye TRAK) were added to the thrombin component. The spray setup was used (0.6 bar and 15 mm nozzle-substrate distance) to create sprayed fibrin constructs (500 μL) on a glass microscope slide. After spraying, gel mixing was evaluated using microscopy (Olympus BX51); images were taken from four random locations in each construct. Microscope images were processed using ImageJ (Version 1.47v). Particle analysis was used to calculate the number of microspheres in the image for each color. The calculated

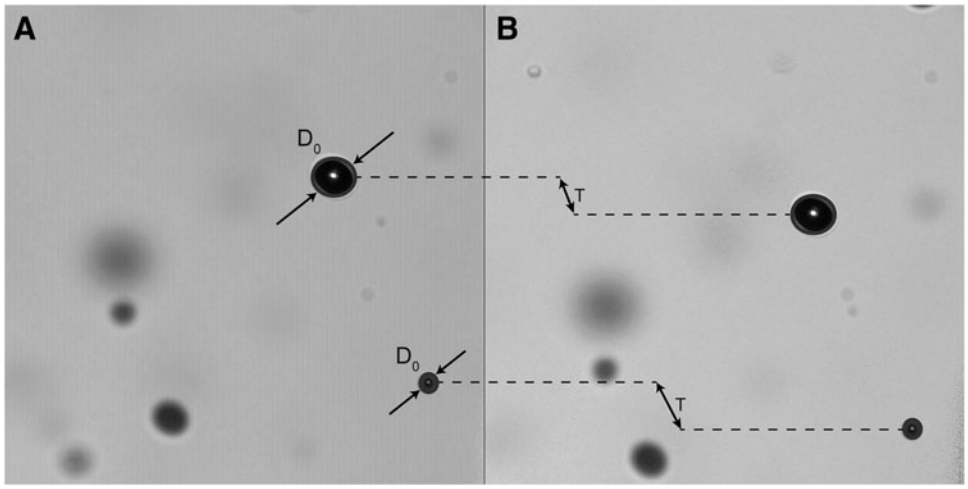

FIG. 3. Representation of two consecutive droplet characterization images. Time delay between **(A, B)** is 1 μs. Droplet diameter is given by D_0, downward *x*-*y* Pythagoras translation of the droplet in $t = 1$ μs is given by *T*. Blurred droplets in **(A, B)** are not detected by the MATLAB script.

amounts were used to calculate the mixing efficiency, described by % mixing, where 100% is considered perfect mixing (equal amounts of microspheres).

Cell isolation and culture

Cartilage was obtained from redundant material from patients who underwent total knee arthroplasty. The anonymous collection of this material was performed according to the Medical Ethical regulations of the University Medical Center Utrecht and the guideline ''good use of redundant tissue for research'' of the Dutch Federation of Medical Research Societies. Articular chondrocytes were isolated using a previously described protocol.[22] Cells were expanded in an expansion medium (Dulbecco's modified Eagle's medium [DMEM; Gibco], 10% fetal bovine serum [FBS; Hyclone, Logan, UT], and 1% Penicillin/Streptomycin [P/S; Gibco, 100 U/mL/100 μg/mL]), passaged at subconfluency, and maintained in the expansion medium until passage 2, when they were harvested for spray experiments.

Bone marrow aspirates were taken from the iliac crest of patients receiving total hip arthroplasty, after their informed consent according to a protocol approved by the local Medical Ethics Committee (University Medical Center Utrecht). Human mesenchymal stromal cells (hMSCs) were isolated from the bone marrow aspirates according to a previously described protocol.[23] Cells were separated on Ficoll-Paque (GE-Healthcare) and the mononuclear fraction was plated for culture in the expansion medium (aMEM [Gibco], 10% FBS, 1% P/S, and 1% L-ascorbic acid-2-phosphate [AsAp; Sigma-Aldrich]). hMSCs were selected based on plastic adherence, as previously described.[24] Cells were passaged at subconfluency and maintained in the expansion medium until passage 3, when they were harvested for spray experiments.

Cell spray setup

The setup shown in Figure 4 was used for cell spray experiments. Two 1 mL syringes (BD Biosciences), either both filled with cells in culture medium or the separated two components of the fibrin glue, were used to push fluid through the spray system. The air pressure was regulated using the DuploSpray pressure regulator, connected to a source of compressed air (0–1.5 bar). The fluid flow was kept as constant as possible.

Cell viability assays

To study cell survival after spraying under the influence of air pressure, cells were sprayed in the expansion medium (DMEM, 10% FBS, and 1% P/S in 12-well plates, 250,000 cells in 500 μL per well), at a distance of 15 mm, using a variable air pressure (0–1.5 bar), in triplicates. After 24 h of culture, relative cell survival was determined by measuring the metabolic activity of the cells using the AlamarBlue assay (10% [w/v] resazurin [Alfa Aesar, Thermo Scientific]). AlamarBlue data were normalized to DNA content and subsequently normalized to the 0 bar samples, resulting in a percentage of relative viability compared to the negative control (0 bar). DNA content was measured using the Quant-IT PicoGreen dsDNA kit (Invitrogen), according to the manufacturer's protocol.

Cell survival after spraying in fibrin glue was determined using a Live/Dead cell viability kit (Molecular Probes; Thermo Scientific). Cells were sprayed in fibrin as cocultures of chondrocytes and hMSCs (ratio 10:90)[25] ($n=2$), in duplicates. When spraying in fibrin glue, cells were dissolved in the fibrinogen component of the fibrin glue at a concentration of 1 million cells per mL, to provide an amount of 250,000 cells per 500 μL fibrin construct. After 72 h of culture, cells were stained using Calcein AM (live cells) and ethidium homodimer-1 (dead cells) in phosphate-buffered saline, as described by the manufacturer. After 30 min of incubation,

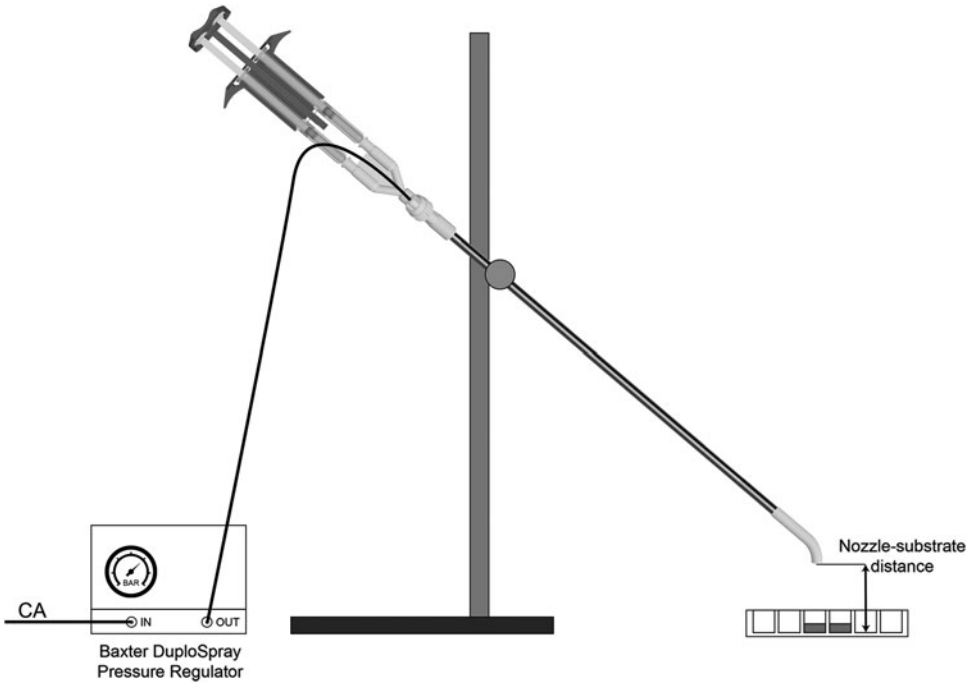

FIG. 4. *In vitro* cell spray setup. The DuploSpray instrument with custom-made or conventional nozzle is stabilized using a stand and clamp, which enables variation of the nozzle-substrate distance. Fluid is pushed through the system with two 1 mL syringes in the Tisseel applicator. Air pressure is supplied by a pressure regulator connected to a source of CA. CA, compressed air.

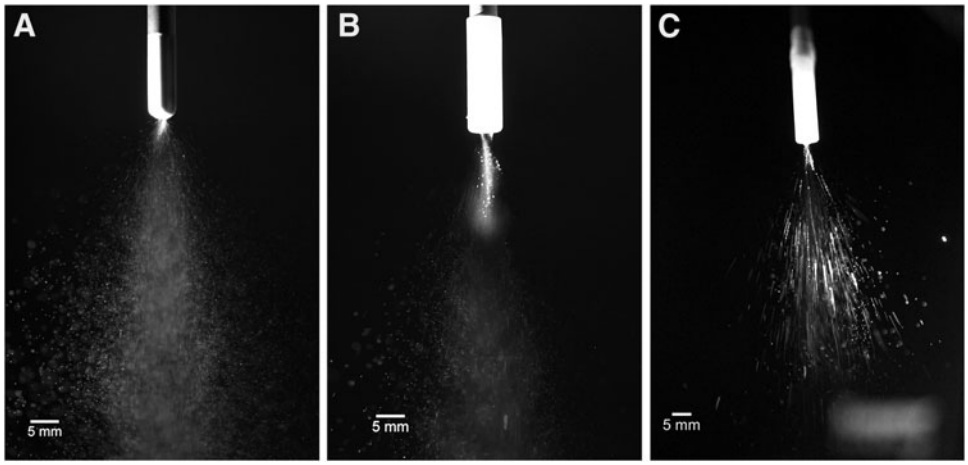

FIG. 5. Spray characterization images captured by conventional photography. **(A–C)** Show the spray pattern of the DuploSpray **(A)**, double barrel **(B),** and 45° double barrel **(C)** nozzle, at a flow rate of 2.4 mL/min and 0.6 bar pressure.

cells were visualized using confocal microscopy (Leica). Two representative images were taken from each fibrin construct.

Chondrogenic gene expression analysis

The influence of cell spraying on the ability of articular chondrocytes to express chondrogenic genes was evaluated using real-time polymerase chain reaction (RT-PCR). Cells were sprayed in 12-well plates, 250,000 cells in 500 μL per well, in DMEM supplemented with 10% FBS, 1% AsAp, and 1% P/S, under varying pressures (0–1.0 bar), using the 45°DB nozzle. After 72 h of culture, total RNA was isolated using Trizol (Invitrogen) as described by the manufacturer. Total RNA (500 ng) was transcribed using the High-Capacity cDNA Reverse Transcription kit (Applied Biosystems). RT-PCRs were performed using iTaq Universal SYBR Green Supermix (Bio-Rad) in a LightCycler 96. RT-PCR was performed for chondrogenic genes, aggrecan (*ACAN*), type II collagen (*COL2A1*), and type I collagen (*COL1A1*). Primer complementary DNA sequences (Invitrogen) were used as a standard, accepting an efficiency of the standard curve >1.85.

Gene expression was analyzed using absolute quantification (LightCycler 96 software) and normalized to *18S* ribosomal RNA (*18S*) expression. Primer sequences (Invitrogen) were as follows: Aggrecan (*ACAN*), Forward: 5′ CAAC TACCCGGCCATCC 3′, Reverse: 5′ GATGGCTCTGTA ATGGAACAC 3′; Type II Collagen (*COL2A1*), Forward: 5′ AGGGCCAGGATGTCCGGCA 3′, Reverse: 5′ GGGTCCC AGGTTCTCCATCT 3′; Type I Collagen (*COL1A1*), Forward: 5′ TCCAACGAGATCGAGATCC 3′, Reverse: 5′ AAGCCGAATTCCTGGTCT 3′, and *18S*; Forward: 5′ GTA ACCCGTTGAACCCCATT 3′, Reverse: 5′ CCATCCAAT CGGTAGTAGCG 3′. The amplified PCR fragments extended over at least one exon border (except for *18S*).[26]

Statistical analysis

Differences in cone angle and width were compared between the three nozzles using an analysis of variance (ANOVA) with Tukey multiple comparisons test. Relative cell viability/DNA after spraying for each air pressure was compared to the 0 bar control using an ANOVA with Dunnett multiple comparisons test. Fold change in relative gene expression for each air pressure was compared to the 0 bar control using an ANOVA with Dunnett multiple comparisons test. A p-value <0.05 was considered statistically significant. GraphPad Prism version 6 was used to perform statistics as well as to generate all graphs.

Results

Development of custom-made spray nozzles

A straight DB nozzle (Fig. 1C) was designed to improve the fibrin mixing and cell survival by changing from internal to external mixing. As many arthroscopic instruments have a 30 or 45° angled tip to improve arthroscopic maneuverability, a 45°DB nozzle was designed (Fig. 1D), which ensures external mixing of the fibrin components and an angled tip to increase arthroscopic maneuverability. The commercially available DuploSpray nozzle (Fig. 1B) was used as a control.

Fluid dynamic analysis: spray pattern characterization

For each nozzle, the cone angle and the cone width at 5, 10, and 15 mm distance to the nozzle were determined (Fig. 5 and Table 1). Although the measured cone angle was relatively similar for all nozzles, the differences between the

Table 1. Spray Characterization

	Cone angle (°)	*Width at 5 mm (in mm)*	*Width at 10 mm (in mm)*	*Width at 15 mm (in mm)*
DuploSpray	24.99 ± 0.86	4.51 ± 0.72	6.70 ± 1.16	8.49 ± 1.12
Double barrel	21.56 ± 1.27	2.74 ± 0.55	4.87 ± 0.47	7.20 ± 0.47
45° double barrel	28.23 ± 2.73	2.98 ± 0.82	5.73 ± 1.30	8.11 ± 1.07

Spray characterization defined by the cone angle and width at 5, 10, and 15 mm distance to the nozzle. Values are given as average ± standard deviation ($N = 10$).

nozzles were statistically significant (Duplo vs. DB: $p=0.0006$, Duplo vs. 45°DB: $p=0.0012$, DB vs. 45°DB: $p<0.0001$). Based on the cone angle measurements, the DB nozzle provided a narrower spray distribution, while the Duplo and 45°DB nozzle were more similar, with 45°DB having the broadest distribution. Differences in cone width were statistically significant at 5 mm for Duplo versus DB: $p<0.0001$ and Duplo versus 45°DB: $p<0.0001$, at 10 mm for Duplo versus DB: $p=0.0015$, and at 15 mm for Duplo versus DB: $p=0.0198$. The cone width measurements confirmed the narrow distribution of the DB nozzle, while the Duplo and 45°DB nozzle provide a broader distribution.

Fluid dynamic analysis: droplet characterization

Droplet characterization was performed using high-speed imaging, providing information on droplet size, velocity, and amounts of detected droplets (droplet density). For the Duplo nozzle, there was a clear distribution of the droplet sizes, identified by smaller droplets in the center of the spray and a gradual increase in droplet size moving toward the edges of the spray (Fig. 6A). With an increasing air pressure, the average droplet size remained similar (Table 2). For the DB nozzle, the distribution of the droplet size was more homogenous compared to the Duplo nozzle, with no distinct increase in droplet size moving toward the edge of the spray, only at 5–10 mm from the center (Fig. 6D). The average droplet size, however, decreased at higher pressures (Table 2). For the 45°DB nozzle, the distribution was heterogeneous, with a clear increase in droplet size at 5–10 mm from the center of the spray (Fig. 6G). The average droplet size gradually decreased with increasing pressure (Table 2). These results indicated that the use of the 45°DB nozzle results in

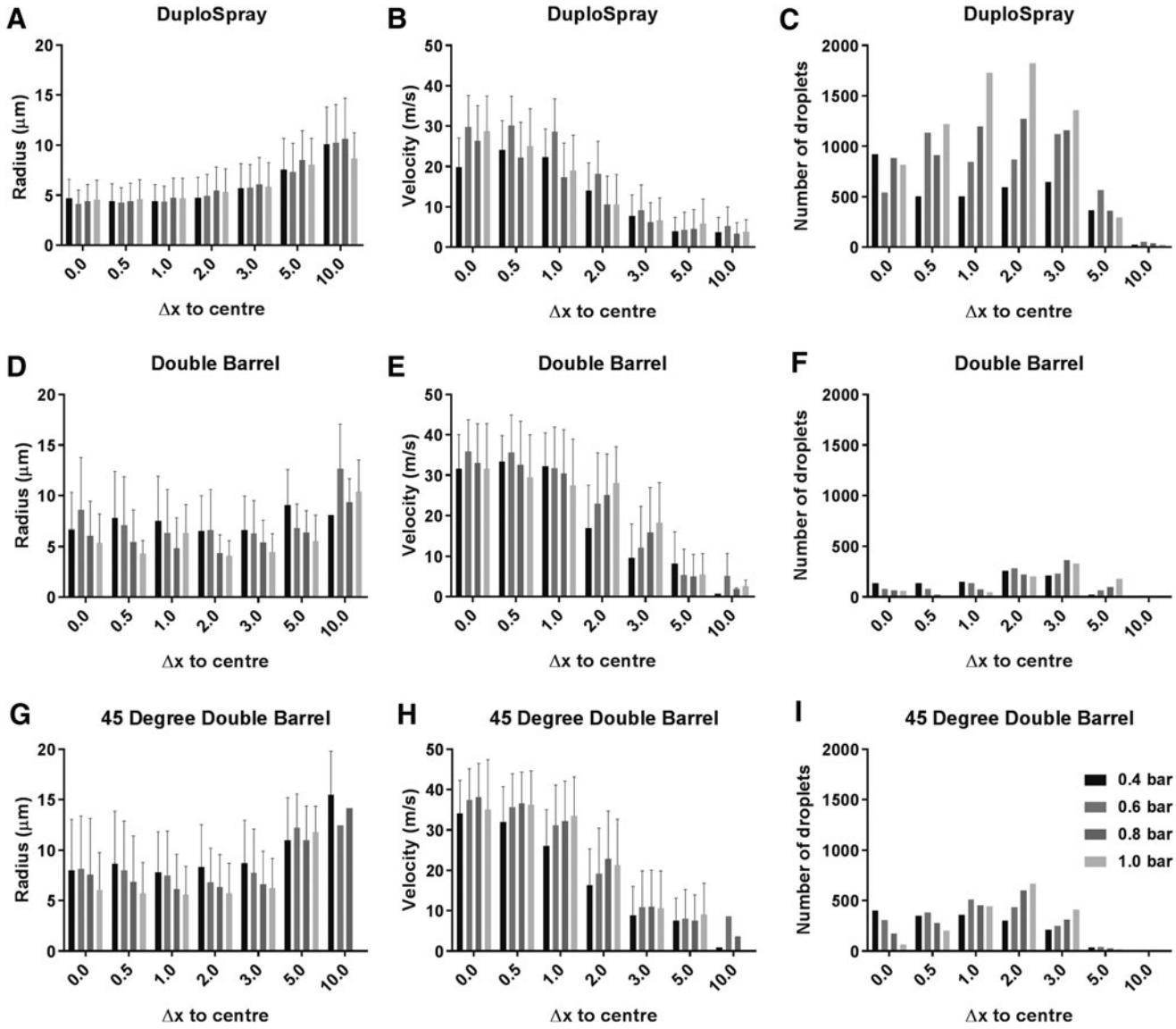

FIG. 6. Droplet characterization. Droplet characterization is defined by droplet radius **(A, D, G)**, velocity **(B, E, H)**, and number of detected droplets **(C, F, I)**. Δx to center on the y-axis indicates the specific location in the spray. Distributions of droplet size, velocity, and density were found to be symmetric; therefore values <0 mm from the center of the spray are not displayed in the graphs. Bar graphs show the mean radius, velocity, or number of droplets, ±SD.

TABLE 2. DROPLET CHARACTERIZATION

	Droplet radius (μm)				*Droplet velocity (m/s)*				*Droplet density (No.)*			
	0.4 bar	*0.6 bar*	*0.8 bar*	*1.0 bar*	*0.4 bar*	*0.6 bar*	*0.8 bar*	*1.0 bar*	*0.4 bar*	*0.6 bar*	*0.8 bar*	*1.0 bar*
DuploSpray	5.65 ± 1.8	5.50 ± 1.9	5.84 ± 2.1	5.60 ± 1.5	14.6 ± 7.7	18.3 ± 10.1	15.82 ± 9.1	17.2 ± 9.7	566 ± 253	785 ± 368	908 ± 425	1091 ± 600
Double barrel	7.18 ± 0.9	7.39 ± 2.0	5.94 ± 1.3	5.64 ± 1.8	19.0 ± 11.6	22.7 ± 12.3	21.4 ± 11.5	21.3 ± 10.7	147 ± 80	167 ± 118	161 ± 128	161 ± 131
45° double barrel	9.21 ± 2.4	8.53 ± 2.06	7.93 ± 2.6	6.75 ± 1.9	21.0 ± 12.3	24.1 ± 12.3	24.7 ± 13.3	26.2 ± 10.8	282 ± 153	336 ± 202	331 ± 266	370 ± 322

Results of the droplet characterization, defined by droplet size (radius), velocity, and droplet density. Values are given as average ± standard deviation.

the largest droplets, while the Duplo nozzle distributed the smallest droplets.

All three nozzles showed a similar trend in terms of droplet velocity; the fastest droplets were detected in the center of the spray with a gradual decrease in velocity toward the edges of the spray (Fig. 6B, E, H). Air pressure was, for most locations in the spray, associated with an increase in droplet velocity (Table 2). For the Duplo nozzle, as is shown in Figure 6B, the air pressure had the highest influence on the droplets located in the center of the spray, resulting in higher velocities. For the DB nozzle, a similar trend was observed, where the fastest droplets were detected in the center or 0.5 mm from the center, with a gradual decrease in velocity toward the edge of the spray (Fig. 6E). For the 45°DB nozzle, the detected velocities were the highest compared to the Duplo and DB nozzle, with the fastest droplets located in the center of the spray (Fig. 6H).

Droplet density is defined as the number of droplets detected in each location of the spray. The number of droplets detected varied significantly between the three nozzles. The number of droplets detected with the Duplo nozzle was higher compared to the DB and 45°DB nozzle (Fig. 6C, F, I, and Table 2). For the Duplo nozzle, no distinct pattern was observed in terms of droplet density. There was, however, a trend toward higher amounts of droplets detected at higher pressures toward the edge of the spray, up to 2 mm from the center of the spray (Fig. 6C). For the DB and 45°DB nozzle, a pattern was observed characterized by lower amounts of droplets detected in the center of the spray and higher amounts of droplets detected toward the edge, up to 2 mm from the center of the spray (Fig. 6F, I). For the Duplo nozzle, the average number of droplets detected was directly influenced by the air pressure (Table 2). For the DB and 45°DB nozzle, this effect was less distinct.

Mixing efficiency

The efficiency of fibrin mixing using the 45°DB nozzle was evaluated using microspheres. Macroscopic evaluation of the images did not show clustering of one of the color microspheres throughout the fibrin constructs, indicating random distribution of the microspheres for both colors (Fig. 7). The particle analyses showed a mixing efficiency of 84.2% ± 3.2%. Using blue microspheres for the fibrinogen component and

FIG. 7. Fibrin mixing efficiency analysis. Blue 15 μm microspheres are shown in *dark gray*, Yellow 15 μm microspheres are shown in *light gray*. Both microspheres were evenly distributed.

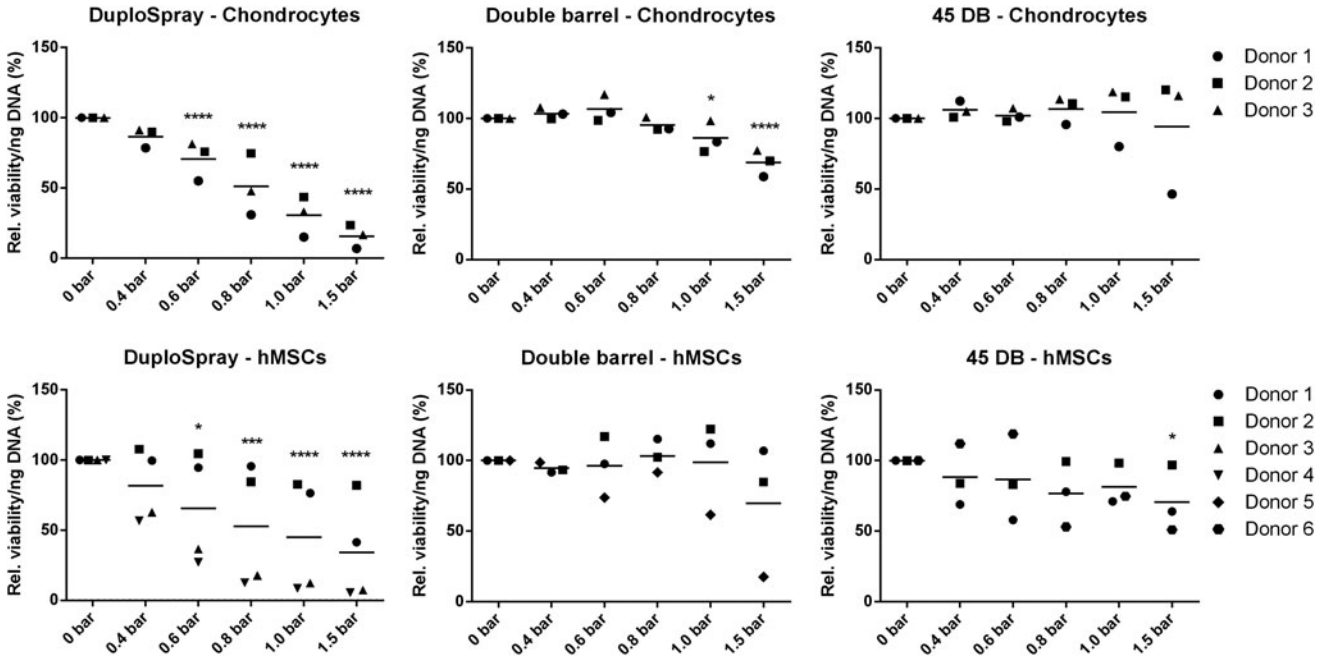

FIG. 8. Relative cell viability 24 h after spraying. Relative cell viability determined by AlamarBlue normalized to DNA content. Donor variability is shown by different data point shapes as indicated in the legend. Mean values are shown for each air pressure. Statistically significant differences compared to the 0 bar control are indicated by *asterisks* (*$p < 0.05$, ***$p < 0.001$, ****$p < 0.0001$). hMSCs, human mesenchymal stromal cells.

yellow microspheres for the thrombin component, or vice versa, showed no significant difference in mixing efficiency (86.5% ± 9.9% vs. 81.9% ± 13.9%).

Cell viability assays

Cell survival after spraying at increasing air pressures was evaluated for human chondrocytes and hMSCs. Using the Duplo nozzle with increasing pressure had a destructive effect on cell survival of both chondrocytes and hMSCs (Fig. 8). The hMSCs showed large donor variability; nevertheless, the overall destructive effect was clearly visible. For chondrocytes, cell viability was significantly decreased at a pressure of 0.6, 0.8, 1.0, and 1.5 bar (70.7% ± 13.1%, 51.1% ± 19.9%, 30.5% ± 13.8%, and 15.73% ± 11.1%, $p < 0.0001$) compared to the 0 bar control. For hMSCs, spraying at 0.6, 0.8, 1.0, and 1.5 bar significantly decreased cell survival (63.4% ± 35.4%, $p = 0.0153$, 50.0% ± 38.9%, $p = 0.0005$, 42.5% ± 36.0%, $p < 0.0001$, and 32.0% ± 32.9%, $p < 0.0001$) compared to the 0 bar control. Using the DB and 45°DB nozzle, minor effects on cell survival were observed when spraying at an increasing pressure. For the DB nozzle, chondrocyte viability was significantly decreased at 1.0 and 1.5 bar (86.1% ± 11.4%, $p = 0.0148$ and 68.7% ± 11.5%, $p < 0.0001$) compared to the 0 bar control. Cell survival of hMSCs was not significantly decreased at increasing pressures. For the 45°DB nozzle, cell survival of chondrocytes was not significantly decreased at any pressure, while survival of hMSCs was significantly decreased at a 1.5 bar pressure (70.6% ± 22.9%, $p = 0.0242$) compared to the 0 bar control.

Cell survival after spraying with the 45°DB nozzle at 0.6 bar in fibrin glue was shown (Fig. 9), which confirms previously described results. The viability after 96 h of culture was 95% for injected samples and 94% for sprayed samples. Spraying in the culture medium as well as fibrin glue at a

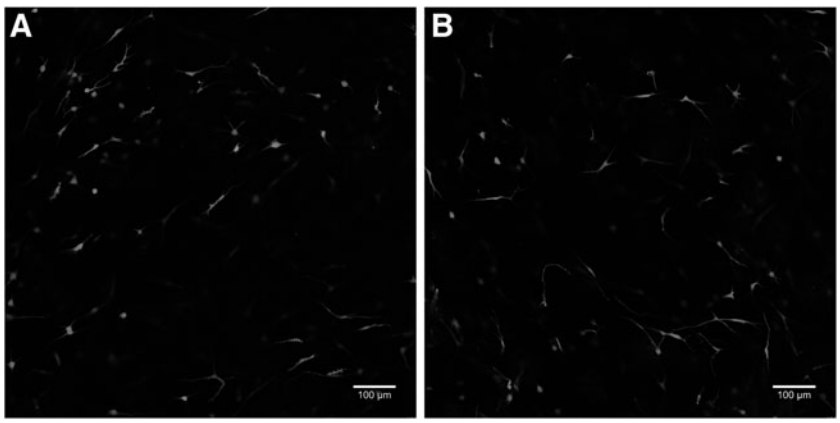

FIG. 9. Live/dead staining for 10:90 cocultures in fibrin glue. **(A)** Shows an injected construct, **(B)** shows a construct sprayed with the 45° double barrel nozzle at 0.6 bar. **(A, B)** Show a viability of >94%.

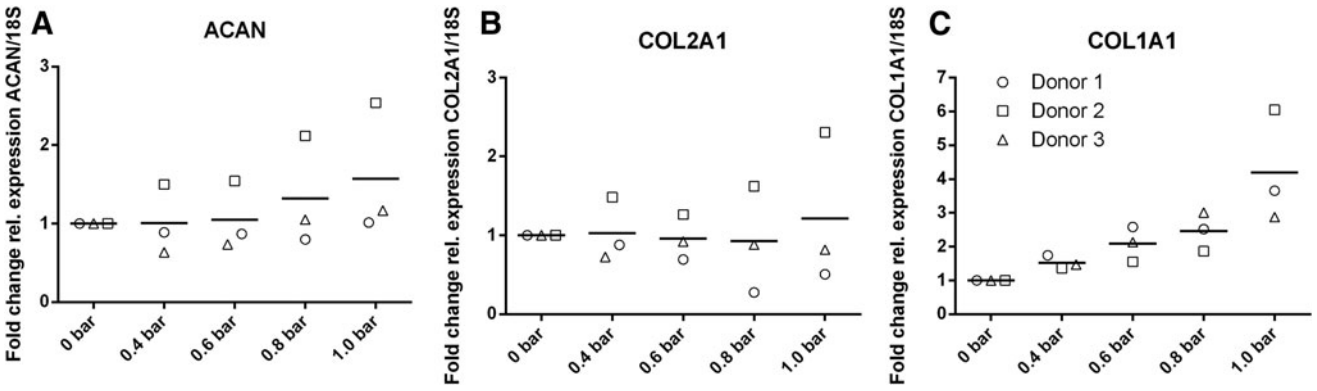

FIG. 10. Chondrogenic gene expression of **(A)** *ACAN*, **(B)** *COL2A1*, and **(C)** *COL1A1* after spraying. Donor variability is shown by different data point shapes, as indicated in the legend. Expression is defined by a fold change in relative expression, compared to the 0 bar control. Mean values are shown for each air pressure. Statistical analysis did not find any statistically significant differences. *ACAN*, aggrecan; *COL2A1*; type II collagen; *COL1A1*, type I collagen.

pressure of 0.6 bar with the 45°DB nozzle did not affect cell survival after spraying.

Chondrogenic gene expression analysis

Chondrogenic gene expression 72 h after spraying at increasing pressures was evaluated for *ACAN*, *COL2A1*, and *COL1A1*. The results display large donor variability, especially for *ACAN* and *COL2A1* (Fig. 10A, B). Overall, no statistically significant effects on gene expression were observed for all chondrogenic genes. For *ACAN*, spraying with a pressure up to 1.0 bar did not affect gene expression, although one donor (donor 2) showed an increased *ACAN* expression at higher pressures (0.8 and 1.0 bar). For *COL2A1*, similar as for *ACAN*, spraying with a pressure up to 1.0 bar did not significantly affect gene expression. A similar trend is observed for one donor (donor 2), characterized by an increased gene expression at higher pressures. *COL1A1* gene expression seemed to show a more distinct trend toward an increased gene expression with increasing air pressure, up to 4.2-fold expression at 1.0 bar (Fig. 10C). The donor variability in *COL1A1* gene expression is evidently smaller than for the other two genes. Nevertheless, the observed trend was shown not to be statistically significant.

Discussion

This study presents a method to optimize spray-applied application of cell therapy products during knee arthroscopy, as well as an extensive study of the fundamental characteristics and feasibility of this technology. Spray-applied cell therapy (with custom-made spray systems) has recently been proposed for a variety of procedures[18,27] and has shown to be easy to use, allows fast gelation, good adherence, and local cellular regeneration.[7,18,28]

The DB and 45°DB nozzle presented in this study are unique in terms of nozzle design compared to the current endoscopic spray technology. Production of custom-made nozzles using 3D printing technology has shown to be feasible for translation of a design into a usable prototype. However, use of these prototypes is limited to *in vitro/ex vivo* use, as the 3D printed material is not strong enough to withstand the forces present during knee arthroscopy, which was confirmed in a pilot experiment in a cadaveric knee.

An important finding of this study is that the type of nozzle chosen for cell spraying significantly affects cell survival. The commercially available DuploSpray nozzle severely decreased cell survival after spraying at an increasing pressure, while high cell survival rates were maintained up to a pressure of 1.0 bar with the custom-made DB and 45°DB nozzle.

During spraying, cells are mainly exposed to two specific events causing significant cell stress that could lead to decreased cell survival; when cells leave the nozzle, they are exposed to shear stress followed by a second event of cell stress, caused by the impact of hitting the target surface. Deformation or subsequent increase of the cell membrane diameter by these stress events can cause cell death.[19,29,30] Nozzle design influences the amount of shear stress that cells experience when leaving the nozzle. By changing the nozzle design from internal mixing to external mixing, it was hypothesized that the shear stress of leaving the nozzle would be significantly decreased, potentially improving cell survival. This could explain the higher survival rates that were observed using the custom-made nozzles.

Alongside nozzle design, assessment of the fundamental characteristics of a spray is essential to provide information about the character of a spray. Spray characteristics defined by the cone angle and width are parameters that are important for successful filling of cartilage defects. Cone width at arthroscopically relevant nozzle-substrate distances (5, 10, and 15 mm) was shown to be smaller than the defect diameter for all nozzles, which makes them usable for the filling of large cartilage defects (17.8 mm diameter, >2.5 cm^2, respectively).

Droplet characteristics such as size, velocity, and density are more fundamental parameters regarding cell survival after spraying. They determine the level of stress experienced at the moment of impact.[19,31] In this study, the largest droplets were observed for the 45°DB nozzle, with an average droplet size ranging from 18.4 to 13.5 μm in diameter (0.4–1.0 bar), compared to the DuploSpray with which the smallest droplets were detected, ranging from 11.3 to 11.2 μm in diameter (0.4–1.0 bar). The assumption is made that cells are centered in the droplet, which would be approximately true for droplet sizes just exceeding the cell size; however, for larger droplets, the cells might be located at the edge of the spreading film where the shear stresses are much higher than in the center.[19,32] The

average cell diameter is 10–15 μm for human chondrocytes[33] and 15–16 μm for hMSCs.[34] In that respect, the 45°DB nozzle produces droplets that are just exceeding the cell diameter and are therefore well suited for spraying of chondrocytes and hMSCs at a pressure of 0.4 and 0.6 bar. Interestingly, detected droplet velocities were the highest for the 45°DB nozzle and smallest for the Duplo nozzle, which is somewhat contradictory because of the inverse correlation with the observed results regarding droplet size. Previously, it was suggested that increasing pressure is associated with smaller droplets at higher velocities, resulting in lower cell survival rates.[19] However, the results of this study suggest that a nozzle producing higher velocity droplets is not directly associated with small droplets and lower cell survival, in case of the 45°DB nozzle.

Viscosity of the spray medium and the substrate stiffness are other parameters determining the level of impact stress and subsequently cell survival. A limitation of the droplet characterization is that these analyses were performed with demi-water. Therefore, it is unknown what the droplet population would resemble when using a spray medium with a higher viscosity, such as fibrin glue. Increasing the droplet viscosity is expected to negatively influence the cell viability. When the viscosity of the droplet would exceed the viscosity of the cell, the cell is expected to dampen the droplet's impact, resulting in significant cell deformation and decreased cell viability.[19] However, in this study, cell survival in the fibrin constructs was shown to be similar to the cell survival rates observed when spraying in the culture medium. Therefore, substrate stiffness and tension might be more important parameters, as a softer substrate provides increased cushioning at the moment of impact.

A possible limitation of this study could be the chosen *in vitro* model for spraying cells. In the cell viability experiments, the substrate stiffness was variable during the procedure. The first layer of sprayed cells was exposed to the plastic substrate of the well plate; thereafter, the substrate stiffness changed to that of the fluid that was used for spraying. In previous studies, viability measurements were performed after spraying a single layer of cells.[18,19] Therefore, the results of this study regarding cell viability are difficult to compare to other studies. However, our experiments do approach the *in vivo* situation, in which the substrate stiffness will also change during spraying. The first layer of cells will hit the subchondral bone inside the defect; thereafter, the following layers of cell-laden fibrin glue will hit the first layers of fibrin glue and mix before complete gelation. Therefore, it is not expected that there will be a layer of damaged cells in the bottom of the filled defect. This was confirmed in a previous study[7] and in the viability experiments in fibrin glue of this study.

Important for successful cartilage regeneration after spraying chondrocytes is that the cells do not lose their chondrogenic capacity. The results of this study indicate that cells retain their capacity to express chondrogenic genes; no significant changes in gene expression of *ACAN*, *COL2A1*, and *COL1A1* were observed due to spraying. However, a trend was observed toward higher *COL1A1* expression when higher air pressures were used, which could indicate an increased dedifferentiation or a fibrocartilaginous phenotype of the chondrocytes.[35] This suggests that air pressure should be carefully regulated and only a specific range of pressures should be used for spraying of chondrocytes, to prevent undesirable dedifferentiation of the cells. In addition, primary cells are preferred above cultivated cells, as they most resemble chondrogenic phenotype.

Conclusions

Custom-made spray nozzles were designed, developed, and characterized, which provide a platform for the development of a BioAirbrush for spray-assisted cell implantations in arthroscopic cartilage repair procedures. Evaluation of the fundamental characteristics of a spray generated by different nozzles, as well as a study of the cell survival after spraying have further expanded the knowledge regarding the most important parameters determining cell survival. Nozzle design, air pressure, and substrate characteristics are essential parameters to consider for the clinical implementation of spray-assisted cell implantations. This work aims at further expanding the knowledge acquired in this study, to eventually enable translation into a clinically approved 45° angled spray instrument for the arthroscopic implantation of cells in cartilage repair procedures.

Acknowledgments

The financial support by the Dutch Arthritis Association is gratefully acknowledged by all authors. The authors wish to thank Alvaro Marin, PhD, and Kirsten Harth, PhD, for their assistance at the Dept. of Physics of Fluids, University of Twente.

Disclosure Statement

No competing financial interests exist.

References

1. Mithoefer, K., Hambly, K., Della Villa, S., Silvers, H., and Mandelbaum, B.R. Return to sports participation after articular cartilage repair in the knee: scientific evidence. Am J Sports Med **37 Suppl 1,** 167S, 2009.
2. Brittberg, M., Lindahl, A., Nilsson, A., Ohlsson, C., Isaksson, O., and Peterson, L. Treatment of deep cartilage defects in the knee with autologous chondrocyte transplantation. N Engl J Med **331,** 889, 1994.
3. Cole, B.J., Pascual-Garrido, C., and Grumet, R.C. Surgical management of articular cartilage defects in the knee. J Bone Joint Surg Am **91,** 1778, 2009.
4. Farr, J., Cole, B., Dhawan, A., Kercher, J., and Sherman, S. Clinical cartilage restoration: evolution and overview. Clin Orthop Relat Res **469,** 2696, 2011.
5. Peterson, L., Vasiliadis, H.S., Brittberg, M., and Lindahl, A. Autologous chondrocyte implantation: a long-term follow-up. Am J Sports Med **38,** 1117, 2010.
6. Biant, L.C., Simons, M., Gillespie, T., and McNicholas, M.J. Cell viability in arthroscopic versus open autologous chondrocyte implantation. Am J Sports Med **45,** 77, 2017.
7. de Windt, T.S., Vonk, L.A., Buskermolen, J.K., Visser, J., Karperien, M., Bleys, R.L.A.W., Dhert, W.J.A., and Saris, D.B.F. Arthroscopic airbrush assisted cell implantation for cartilage repair in the knee: a controlled laboratory and human cadaveric study. Osteoarthritis Cartilage **23,** 143, 2015.
8. Shetty, A.A., Kim, S.J., Shetty, V., Stelzeneder, D., Shetty, N., Bilagi, P., and Lee, H.-J. Autologous bone-marrow mesenchymal cell induced chondrogenesis: single-stage arthroscopic cartilage repair. Tissue Eng Regen Med **11,** 247, 2014.
9. Cole, B.J., Farr, J., Winalski, C.S., Hosea, T., Richmond, J., Mandelbaum, B., and De Deyne, P.G. Outcomes after a

single-stage procedure for cell-based cartilage repair: a prospective clinical safety trial with 2-year follow-up. Am J Sports Med **39,** 1170, 2011.
10. Whyte, G.P., Gobbi, A., and Sadlik, B. Dry arthroscopic single-stage cartilage repair of the knee using a hyaluronic acid-based scaffold with activated bone marrow-derived mesenchymal stem cells. Arthrosc Tech **5,** e913, 2016.
11. Shetty, A.A., Kim, S.J., Bilagi, P., and Stelzeneder, D. Autologous collagen-induced chondrogenesis: single-stage arthroscopic cartilage repair technique. Orthopedics **36,** e648, 2013.
12. de Windt, T.S., Vonk, L.A., Slaper-Cortenbach, I.C.M., van den Broek, M.P.H., Nizak, R., van Rijen, M.H.P., de Weger, R.A., Dhert, W.J.A., and Saris, D.B.F. Allogeneic mesenchymal stem cells stimulate cartilage regeneration and are safe for single-stage cartilage repair in humans upon mixture with recycled autologous chondrons. Stem Cells **35,** 256, 2017.
13. Allouni, A., Papini, R., and Lewis, D. Spray-on-skin cells in burns: a common practice with no agreed protocol. Burns **39,** 1391, 2013.
14. Gravante, G., Di Fede, M.C., Araco, A., Grimaldi, M., De Angelis, B., Arpino, A., Cervelli, V., and Montone, A. A randomized trial comparing ReCell system of epidermal cells delivery versus classic skin grafts for the treatment of deep partial thickness burns. Burns **33,** 966, 2007.
15. Chua, A.W.C., Khoo, Y.C., Tan, B.K., Tan, K.C., Foo, C.L., and Chong, S.J. Skin tissue engineering advances in severe burns: review and therapeutic applications. Burn Trauma **4,** 3, 2016.
16. Falanga, V., Iwamoto, S., Chartier, M., Yufit, T., Butmarc, J., Kouttab, N., Shrayer, D., and Carson, P. Autologous bone marrow-derived cultured mesenchymal stem cells delivered in a fibrin spray accelerate healing in murine and human cutaneous wounds. Tissue Eng **13,** 1299, 2007.
17. Kirsner, R.S., Marston, W.A, Snyder, R.J., Lee, T.D., Cargill, D.I., and Slade, H.B. Spray-applied cell therapy with human allogeneic fibroblasts and keratinocytes for the treatment of chronic venous leg ulcers: a phase 2, multicentre, double-blind, randomised, placebo-controlled trial. Lancet **380,** 977, 2012.
18. Thiebes, A.L., Reddemann, M.A., Palmer, J., Kneer, R., Jockenhoevel, S., and Cornelissen, C.G. Flexible endoscopic spray application of respiratory epithelial cells as platform technology to apply cells in tubular organs. Tissue Eng Part C Methods **22,** 322, 2016.
19. Hendriks, J., Willem Visser, C., Henke, S., Leijten, J., Saris, D.B.F., Sun, C., Lohse, D., and Karperien, M. Optimizing cell viability in droplet-based cell deposition. Sci Rep **5,** 11304, 2015.
20. Ho, C.M.B., Ng, S.H., Li, K.H.H., and Yoon, Y.-J. 3D printed microfluidics for biological applications. Lab Chip **15,** 3627, 2015.
21. Lee, J.M., Zhang, M., and Yeong, W.Y. Characterization and evaluation of 3D printed microfluidic chip for cell processing. Microfluid Nanofluidics **20,** 5, 2016.
22. Vonk, L.A., Kragten, A.H.M., Dhert, W.J.A., Saris, D.B.F., and Creemers, L.B. Overexpression of hsa-miR-148a promotes cartilage production and inhibits cartilage degradation by osteoarthritic chondrocytes. Osteoarthritis Cartilage **22,** 145, 2014.
23. Gawlitta, D., van Rijen, M.H.P., Schrijver, E.J.M., Alblas, J., and Dhert, W.J.A. Hypoxia impedes hypertrophic chondrogenesis of human multipotent stromal cells. Tissue Eng Part A **18,** 1957, 2012.
24. Dominici, M., Le Blanc, K., Mueller, I., Slaper-Cortenbach, I., Marini, F., Krause, D., Deans, R., Keating, A., Prockop, D., and Horwitz, E. Minimal criteria for defining multipotent mesenchymal stromal cells. The International Society for Cellular Therapy position statement. Cytotherapy **8,** 315, 2006.
25. Bekkers, J.E.J., Tsuchida, A.I., van Rijen, M.H.P., Vonk, L.A., Dhert, W.J.A., Creemers, L.B., and Saris, D.B.F. Single-stage cell-based cartilage regeneration using a combination of chondrons and mesenchymal stromal cells: comparison with microfracture. Am J Sports Med **41,** 2158, 2013.
26. Vonk, L.A., Kroeze, R.J., Doulabi, B.Z., Hoogendoorn, R.J., Huang, C., Helder, M.N., Everts, V., and Bank, R.A. Caprine articular, meniscus and intervertebral disc cartilage: an integral analysis of collagen network and chondrocytes. Matrix Biol **29,** 209, 2010.
27. Fortelny, R.H., Petter-Puchner, A.H., Khakpour, Z., May, C., Mika, K., Glaser, K. S., and Redl, H. Spray application of fibrin sealant with an angled spray tip device in laparoscopic inguinal hernia repair. Eur Surg **42,** 171, 2010.
28. Zimmerlin, L., Rubin, J.P., Pfeifer, M.E., Moore, L.R., Donnenberg, V.S., and Donnenberg, A.D. Human adipose stromal vascular cell delivery in a fibrin spray. Cytotherapy **15,** 102, 2013.
29. Tasoglu, S., Kaynak, G., Szeri, A.J., Demirci, U., and Muradoglu, M. Impact of a compound droplet on a flat surface: a model for single cell epitaxy. Phys Fluids (1994) **22,** 82103, 2010.
30. Barbee, K.A. Mechanical cell injury. Ann N Y Acad Sci **1066,** 67, 2005.
31. Tirella A., and Ahluwalia, A. The impact of fabrication parameters and substrate stiffness in direct writing of living constructs. Biotechnol Prog **28,** 1315, 2012.
32. Visser, C.W., Frommhold, P.E., Wildeman, S., Mettin, R., Lohse, D., and Sun, C. Dynamics of high-speed micro-drop impact: numerical simulations and experiments at frame-to-frame times below 100 ns. Soft Matter **11,** 1708, 2015.
33. Guilak, F., Erickson, G.R., and Ting-Beall, H.P. The effects of osmotic stress on the viscoelastic and physical properties of articular chondrocytes. Biophys J **82,** 720, 2002.
34. Heathman, T.R.J., Glyn, V.A.M., Picken, A., Rafiq, Q.A., Coopman, K., Nienow, A.W., Kara, B., and Hewitt, C.J. Expansion, harvest and cryopreservation of human mesenchymal stem cells in a serum-free microcarrier process. Biotechnol Bioeng **112,** 1696, 2015.
35. Schnabel, M., Marlovits, S., Eckhoff, G., Fichtel, I., Gotzen, L., Vécsei, V., and Schlegel, J. Dedifferentiation-associated changes in morphology and gene expression in primary human articular chondrocytes in cell culture. Osteoarthr Cartil **10,** 62, 2002.

Address correspondence to:
Daniel B. Saris, MD, PhD
Department of Orthopaedics
University Medical Center Utrecht
Heidelberglaan 100 (POB G05.228)
Utrecht 3584 CX
The Netherlands

E-mail: d.saris@umcutrecht.nl

Received: April 26, 2017
Accepted: June 27, 2017
Online Publication Date: August 8, 2017